RESEARCH ARTICLE

AMERICAN JOURNAL OF medical genetics PART A

The Fetal Brain Transcriptome and Neonatal Behavioral Phenotype in the Ts1Cje Mouse Model of Down syndrome

Faycal Guedj,[1]* Jeroen L. A. Pennings,[2] Millie A. Ferres,[1] Leah C. Graham,[1] Heather C. Wick,[3] Klaus A. Miczek,[4] Donna K. Slonim,[3] and Diana W. Bianchi[1]*

[1]Mother Infant Research Institute, Tufts Medical Center and the Floating Hospital for Children, Boston, Massachusetts

[2]Center for Health Protection (GZB), National Institute for Public Health and the Environment (RIVM), Bilthoven, The Netherlands

[3]Department of Computer Science, Tufts University, Medford, Massachusetts

[4]Department of Psychology, Tufts University, Medford, Massachusetts

Manuscript Received: 26 November 2014; Manuscript Accepted: 27 April 2015

Human fetuses with Down syndrome demonstrate abnormal brain growth and reduced neurogenesis. Despite the prenatal onset of the phenotype, most therapeutic trials have been conducted in adults. Here, we present evidence for fetal brain molecular and neonatal behavioral alterations in the Ts1Cje mouse model of Down syndrome. Embryonic day 15.5 brain hemisphere RNA from Ts1Cje embryos (n = 5) and wild type littermates (n = 5) was processed and hybridized to mouse gene 1.0 ST arrays. Bioinformatic analyses were implemented to identify differential gene and pathway regulation during Ts1Cje fetal brain development. In separate experiments, the Fox scale, ultrasonic vocalization and homing tests were used to investigate behavioral deficits in Ts1Cje pups (n = 29) versus WT littermates (n = 64) at postnatal days 3–21. Ts1Cje fetal brains displayed more differentially regulated genes (n = 71) than adult (n = 31) when compared to their age-matched euploid brains. Ts1Cje embryonic brains showed up-regulation of cell cycle markers and down-regulation of the solute-carrier amino acid transporters. Several cellular processes were dysregulated at both stages, including apoptosis, inflammation, Jak/Stat signaling, G-protein signaling, and oxidoreductase activity. In addition, early behavioral deficits in surface righting, cliff aversion, negative geotaxis, forelimb grasp, ultrasonic vocalization, and the homing tests were observed. The Ts1Cje mouse model exhibits abnormal gene expression during fetal brain development, and significant neonatal behavioral deficits in the pre-weaning period. In combination with human studies, this suggests that the Down syndrome phenotype manifests prenatally and provides a rationale for prenatal therapy to improve perinatal brain development and postnatal neurocognition. © 2015 Wiley Periodicals, Inc.

Key words: Down syndrome; embryonic brain; systems biology; gene expression; neonatal behavior; genotype/phenotype correlation

How to Cite this Article:
Guedj F, Pennings JLA, Ferres MA, Graham LC, Wick HC, Miczek KA, Slonim DK, Bianchi DW. 2015. The Fetal Brain Transcriptome and Neonatal Behavioral Phenotype in the Ts1Cje Mouse Model of Down syndrome.
Am J Med Genet Part A 167A:1993–2008.

Conflict of interest: none.
Author contributions: Drs. Guedj and Bianchi had full access to all of the data in the study and take responsibility for the integrity of the data and the accuracy of the data analysis. Study concept and design: Guedj, Bianchi. Acquisition of data: Guedj, Ferres, Graham. Analysis and Interpretation of Data: Guedj, Pennings, Wick, Bianchi. Drafting of the manuscript: Guedj, Pennings, Bianchi. Critical revision of the manuscript for important intellectual content: Bianchi, Guedj, Pennings, Slonim, Miczek. Statistical Analysis: Wick, Pennings, Guedj. Final approval of the version to be published: Guedj, Pennings, Wick, Bianchi, Ferres, Graham, Miczek, Slonim. Obtained funding: Bianchi. Study supervision: Bianchi.
Grant sponsor: Verinata Health, Inc., an Illumina company, and the Eunice Kennedy Shriver National Institute of Child Health and Human Development; Grant number: R01HD058880-01.
*Correspondence to:
Faycal Guedj, Ph.D. and Diana W. Bianchi, M.D., Mother Infant Research Institute, Tufts Medical Center and the Floating Hospital for Children, Boston, MA.
E-mail: faycal.guedj@tufts.edu (F.G); dbianchi@tuftsmedicalcenter.org (D.W.B.)
Article first published online in Wiley Online Library (wileyonlinelibrary.com): 14 May 2015
DOI 10.1002/ajmg.a.37156

INTRODUCTION

The neurocognitive disabilities associated with Down syndrome (DS) are increasingly the target of therapeutic research [Guedj et al., 2014]. Most clinical trials are focused on adolescents and adults with DS. Changes in brain morphogenesis in affected individuals are, however, already recognizable during fetal life [Winter et al., 2000; Guihard-Costa et al., 2006]. We hypothesize that a potential window of opportunity exists in which to treat pregnant women carrying fetuses diagnosed with DS in the first trimester [Guedj and Bianchi, 2013].

The molecular origin of brain alterations that occur prenatally in fetuses with DS is poorly understood. Only two studies have investigated gene expression changes in fetal brains, but these were performed on post-mortem tissue [Mao et al., 2003; Mao et al., 2005]. To circumvent the limited access to human samples, other studies have investigated transcriptome differences in cultured neural progenitor cells derived from affected post-mortem human fetal brains or amniotic fluid cell-free RNA [Esposito et al., 2008; Slonim et al., 2009; Weick et al., 2013]. Multiple processes affecting brain development and function were shown to be dysregulated in these samples, including neurogenesis, GABAR activity, ion transport, G-protein signaling, oxidative stress, and apoptosis.

While some published gene expression data from early postnatal and adult brain tissue from the Ts1Cje and Ts65Dn mouse models of DS found several pathway changes similar to what has been observed in humans [Saran et al., 2003; Amano et al., 2004; Kahlem et al., 2004; Laffaire et al., 2009; Ling et al., 2014], fetal and neonatal phenotypic changes in DS mouse models have not been extensively studied. It is also unknown how fetal and neonatal molecular changes affect developmental milestones and early postnatal behavior in mouse models of DS. Thus, investigating both fetal brain molecular abnormalities in conjunction with neonatal and adult behavioral changes provides not only more insight into the origin of the adult DS phenotype, but also identifies endpoints to evaluate the effects of prenatal treatment.

We have previously described whole transcriptome changes in the adult cerebral cortex and hippocampus of Ts1Cje mice, and identified functional abnormalities and pathways that can be targeted for effective therapeutic strategies to improve cognitive outcome in DS [Guedj et al., 2015]. Here, we investigated gene expression changes in the embryonic brains of day 15.5 Ts1Cje mice and compared them to wild-type (WT) embryonic brains to investigate the molecular origin of the fetal brain phenotype in DS. We also compared the transcriptomic analyses to the previous studies of adult Ts1Cje cortex and hippocampus. To understand how early molecular changes affect the postnatal cognitive outcome in DS, we explored the pre-weaning phenotype of Ts1Cje pups using a comprehensive set of neonatal behavioral tests.

MATERIALS AND METHODS

Embryo Dissection and Genotyping

All experiments were conducted according to international ethical standards and approved by the Institutional Animal Care and Use Committee (IACUC) of Tufts University (Protocol B2013-20). Mice were housed in standard cages with food and water ad libitum under a controlled environment (temperature = 20°C; humidity = 60%) and a light/dark cycle of 12 hr. Ts1Cje males (on a C57Bl/6J background) were crossed with C57Bl/6J females (Jackson Laboratories, Bar Harbor, ME) and the presence of a vaginal plug was defined as embryonic day 0.5 (E0.5) and 10% weight gain at embryonic day 10 as described previously [Johnson et al., 2010]. Pregnant females were anesthetized with 2.5% isoflurane in a 3/7 $0_2/N_2O$ mixture and euthanized by decapitation at embryonic day E15.5 (E15.5). Embryos were extracted, identified as ST23 (E15.5) using Theiler staging (http://www.emouseatlas.org) and decapitated in ice-cold phosphate-buffered-saline (PBS1X). Embryonic brains were rapidly removed and brain hemispheres dissected on a cold platform and snap frozen in liquid nitrogen before storage at −80°C.

Genomic DNA was purified from embryonic tails using a standard isopropanol precipitation protocol without the NaCl protein precipitation step [Guedj et al., 2012]. Genotyping was carried out on 100 ng of genomic DNA using the multiplex PCR protocol previously described [Olson et al., 2004]. PCR products were subjected to 2% agarose gel electrophoresis and visualized under UV light. Ts1Cje mice were identified by the presence of the 270 bp neomycin cassette amplicon.

Embryonic Brain RNA Isolation and Microarray Experiments

Total RNA was isolated from brain hemispheres of Ts1Cje E15.5 embryos (n = 5) and their wild-type littermates (n = 5) using the RNA II kits, following the manufacturer's instructions (Macherey-Nagel, Bethlehem, PA). RNA concentrations were measured as absorbance at 260 nm and RNA quality was analyzed with the Bioanalyzer (Agilent Biotechnologies, Santa Clara, CA). Samples with an A260/A280 ratio of 2.0–2.1 and a RIN (RNA Integrity Number) >9 were used for array hybridization experiments.

RNA was processed for hybridization to Affymetrix mouse gene 1.0 ST arrays (Affymetrix, Santa Clara, CA) as described previously [Guedj et al., 2015]. A total of ten arrays were used (5 Ts1Cje and 5 WT), and each array corresponded to labeled RNA from one individual embryo. Analyses were performed as described previously [Guedj et al., 2015] using Benjamini-Hochberg False Discovery Rate (BH-FDR) of 20% as a cut-off [Benjamini and Hochberg, 1995]. Statistical analyses were carried out on the normalized data using R software (version 2.13.1) unless indicated otherwise. Gene expression data from WT and Ts1Cje tissues were compared using an unpaired t-test. Gene expression data were further visualized in R by means of a heatmap (R-package 'stats') combined with hierarchical clustering (Euclidean distance metric, Ward linkage).

Functional analyses were performed using the Gene Set Enrichment Analysis (GSEA) [Subramanian et al., 2005] and the Database for Annotation, Visualization, and Integrated Discovery (DAVID) [Huang et al., 2009]. We used the top 1% up-and down-regulated genes (424 genes) in the Ts1Cje embryonic brains versus age-matched WT controls for DAVID analysis, and transcriptional data across the entire microarrays as input for functional analyses using the GSEA and DFLAT databases. Gene sets were considered

differentially regulated if the GSEA or DAVID P value was <0.05. Both the *Sod1* and *Dnahc11* genes were excluded from subsequent pathway analyses as they represent abnormal loci in the Ts1Cje mouse model [Guedj et al., 2015].

Quantitative real-time PCR amplification was used to confirm the microarray data. Several genes, including *Dyrk1A*, *Rcan1*, *Cyb5r1*, *Tsga10*, *Cdc25*, and *Slc6A9*, were amplified. Reverse transcription was performed using the Retroscript kit® with 1.5 μg of total RNA according to the manufacturer's instructions (Life Technologies, Grand Island, NY). Gene expression was analyzed using 100 ng of cDNA added to the PCR mixture (TaqMan gene expression 2X and TaqMan gene expression assay 20X) for a final volume of 20 μl in 96-well plate according to the TaqMan protocol (Life Technologies). PCR amplification was conducted on the Quant-Studio 7 Real-Time PCR System (Life Technologies). The TaqMan gene expression assays used are listed in Supplemental Methods. Amplification plots and predicted threshold cycle (Ct) values were obtained with the Sequence Detection Software (SDS 2.2, Applied Biosystems). Data were analyzed using the ΔΔCt relative quantification method and mean expression ratios from Ts1Cje ($n = 12$) and WT ($n = 10$) embryos were compared using beta-actin (*β-actin*) and glyceraldehyde-3-phosphate dehydrogenase (*Gapdh*) as housekeeping genes.

Developmental Milestones and Neonatal Behavior Assessment

Ts1Cje pups and their WT littermates from both sexes were subjected to a comprehensive set of neonatal behavior tests, including the Fox scale, ultrasonic vocalization (USV) and the homing test to measure different cognitive, sensory and motor development parameters between postnatal days 3 and 21 (P3 to P21).

During the testing period, when the pups were separated from the dam, they were placed with nesting material in a small bowl positioned on a heating pad at 37°C. A heat lamp was also placed over the mice to provide heat from above. All neonatal neurobehavioral tests were performed blindly without prior knowledge of genotype.

Developmental Milestones

We used a modified version of the Fox scale as described by Hill et al. (2008) to investigate developmental milestones in Ts1Cje neonates ($n = 29$) versus WT littermates ($n = 64$). The Fox scale is a battery of tests that measure: (1) body righting and coordination (surface righting, air righting and negative geotaxis), (2) strength (cliff aversion and forelimb grasp), (3) sensory system maturation (rooting, auditory startle, ear twitch, and eye opening), (4) and extinction of rotatory behavior (open field) [Fox, 1965; Hill et al., 2008]. Ts1Cje pups and their age-matched controls were evaluated on a daily basis starting at P3 and ending on either day P15.5 when eye opening occurred or day P21 at weaning. The experiments started on day P3 to avoid maternal stress and cannibalism during the first two days after birth, a phenomenon observed in our preliminary pilot experiments. The amount of time (latency) needed to complete each test was recorded and analyzed. Detailed protocols for the different neurobehavioral tests used are described in the Supplemental Methods section.

Ultrasonic Vocalization

The ultrasonic vocalization test is a standard technique used to measure communication skills and anxiety levels in rodents when subjected to an external stress or stimuli. This test is widely used to evaluate early postnatal neurocognitive outcome in mouse models of autism or to investigate the effects of a particular treatment on brain development and behavior [Covington and Miczek, 2003; Takahashi et al., 2009; Wohr and Scattoni, 2013].

At postnatal day 8, Ts1Cje ($n = 13$) and WT ($n = 18$) pups were separated from their dams for 25 min, then individually tested for 1 min in the ultrasonic vocalization chamber at 16°C as described previously [Dirks et al., 2002]. After the first screening trial, pups were moved back to a small bowl positioned on a heating pad at 37°C, separated from their mother for 20 min, then re-tested in a second trial for 5 min. The number of USVs uttered by each pup in each session was recorded using a high frequency condenser microphone (Bruel and Kiaer, Naerum, Danmark), amplified and analyzed with Sonotrack software (Metris, Hoofddorp, Netherlands).

During the second trial, locomotor activity in Ts1Cje and WT pups was analyzed by estimating the number of grid crossings and body rolls on the testing platform (30 cm^2) divided into a 2.5 cm^2 grid.

Homing Test

In this test, olfactory-based spatial memory was assessed before eye-opening in Ts1Cje ($n = 12$) and WT ($n = 16$) neonates as described previously [Santucci et al., 1993]. At postnatal day 12, pups were separated from their dams for 30 min before testing, and transferred to a clean cage containing new nesting material in a separate testing room. Individual pups were then transferred to the testing Plexi-glass arena ($36 \times 22.5 \times 10$ cm) maintained at 30°C, in which wood shavings from the home cage were evenly spread under the wire-mesh floor on one side of the arena (12×22.5 cm, goal area).

For testing, each pup was placed close to the wall on the opposite side of the goal area. The time taken by Ts1Cje and WT neonates to reach the goal area was recorded during a three-minute trial period. Each pup was subjected to two trials with an inter-trial interval of 60 min. Animals that did not reach the goal area after three minutes were assigned the maximum latency (180 sec).

Statistical Analysis

Prior to choosing the appropriate statistical test, we performed the Kolmogorov–Smirnov normality test and the Fisher variance equality test. In case both Ts1Cje and WT populations followed a normal distribution and have similar variances, parametric Student or ANOVA tests were used. In the opposite situation, non-parametric rank based tests (Mann–Whitney and Wilcoxon tests), which do not make these assumptions and have higher statistical power with large populations such as ours, were performed. Appropriate statistical tests were used for single and repeated measures, respectively, to determine significant differences between the WT and Ts1Cje groups at a P value of 0.05. Graphs were plotted as Mean ± SEM and all statistical analyses

were performed using the GraphPad Prism 6.0 software package (GraphPad Software, Inc, La Jolla, CA).

RESULTS

Transcriptomic Changes Are Already Present in Ts1Cje Embryonic Brains

When compared to their WT littermates, brains from Ts1Cje E15.5 embryos displayed 71 statistically significantly differentially expressed genes (65 up-regulated, six down-regulated) (Table I). Thirty-nine of the differentially expressed genes mapped to the MMU16 trisomic region (Table I). Four genes (*Dnahc11*, *Itgb8*, *Sp4*, and *Sp8*) were located on the MMU12 monosomic region (Table I). Almost half of the differentially regulated genes (28/71) were present in two copies in the Ts1Cje mice (Table I). Among these, 25 were up-regulated and three (*Sppl3*, *Tle2*, and *Rfx5*) were down-regulated.

Transcriptomic Changes in Embryonic versus Adult Brain. Comparison of gene expression changes in the Ts1Cje embryonic day 15.5 (E15.5) brains with our previously published adult cerebral cortex and hippocampus datasets (GSE49635) revealed that transcriptional dysregulation was more pronounced in the embryonic Ts1Cje brain (Fig. 1). Seventy-one genes were dysregulated in the Ts1Cje embryonic brain hemispheres, while only 30 (25 up-regulated, five down-regulated) were dysregulated in the adult hippocampus, seven (six up-regulated, one down-regulated) in the adult cortex; six were dysregulated in both tissues. In total, the expression of eighty genes was perturbed at E15.5 and/or adulthood in the Ts1Cje brains at an FDR of 20% (Fig. 1, Table SI). Even if differential gene expression of regulated genes reached statistical significance in just one tissue, the direction of their regulation (up or down) was largely consistent in all tissues examined, particularly between the E15.5 brains and the cerebral cortex (Fig. 2).

For the 77 MMU16 genes that are present in three copies in Ts1Cje, 22 were dysregulated in the adult cortex and/or hippocampus, whereas 39 genes were significantly up-regulated in embryonic brain (Table SI). Among these genes, four (i.e., *Gart*, *Rcan1*, *Synj1*, and *Dyrk1A*) were statistically significantly differentially expressed in both embryonic and adult Ts1Cje brains.

In Silico Functional Pathway Analyses in Ts1Cje Embryonic Brain

Up-regulation of pro-cell cycle markers in the Ts1Cje embryonic brain. Functional analysis of the top 1% up-regulated genes (Table SII) identified thirty genes associated with several terms related to cell cycle in the Ts1Cje embryonic brain. Multiple genes are known to play a major role in mitosis regulation, including cyclin B2 (*Ccnb2*), cell division cycle associated genes two and three (*Cdc2*, *Cdc3*), polo-like kinase 1 (*Plk1*) and cyclin dependent kinase 1 (*Cdk1*) (Tables II and III).

Other genes, including *Bub1*, *Kif11*, *Zwilch*, *Nusap1*, *Kif4*, and *Kif15* that regulate spindle assembly and kinetochore formation were also up-regulated in the Ts1Cje E15.5 brain (Tables II and III). Additionally, Gene Ontology (GO) categories closely related to cell cycle regulation, such as chromosome organization, nucleosome organization, histone core and microtubule cytoskeleton organization were enriched in the top 1% up-regulated gene list from the Ts1Cje embryonic brain (Table II).

Down-regulation of SLC-mediated amino-acid transport in Ts1Cje embryonic brains. Functional analysis on the top 1% down-regulated genes (Table SII) in the Ts1Cje E15.5 brains revealed enrichment of solute carrier (SLC)-amino acid transmembrane transporters. Eight annotated SLC-amino acid transporter genes (*Slc1a4*, *Slc6a9*, *Slc6a11*, *Slc7a3*, *Slc25a18*, *Slc3a2*, *Slc7a1*, and *Slc7a5*) were down-regulated and only one (*Slc6a4*) was up-regulated (Tables II and SII). Dysregulation of SLC genes include transporters involved in glutamate recycling or NMDAR activation (*Slc1a4*, *Slc6a9*, and *Slc7a3*), serotonin reuptake (*Slc6a4* and *Slc25a18*) or L-Dopa transport (*Slc3a2* and *Slc7a5*). Four other differentially regulated SLC genes were implicated in bicarbonate transport (*Slc4a1*, *Slc4a5*), Na+/myo-inositol co-transport (*Slc5A3*) or mitochondrial iron transport (*Slc25a37*) (Table SII).

Commonalities between Ts1Cje embryonic and adult brains. Functional analyses identified a number of common pathways and cellular processes that were consistently dysregulated in both Ts1Cje embryonic and adult brains when compared to their respective littermate controls.

Neurological system processes (cognition and behavior), G-protein coupled receptor protein signaling, particularly olfactory receptor activity, as well as mRNA translation, were down-regulated at both stages. Some changes were mainly observed in the embryonic brains such as MHC class I complex-dependent antigen processing and presentation, cell adhesion and oxidoreductase activity via NAD, and NADP (Table II). GSEA analysis also highlighted down-regulation of terms related to potassium channel and GABAR and NMDAR activation (Table III).

In contrast to the Ts1Cje E15.5 brain, cell cycle-related categories were not significantly affected in Ts1Cje adult brain cortex compared to littermate controls. Most up-regulated pathways were shared between these two tissues, including phosphorus metabolic processes (i.e., kinase activity), apoptosis, and MHC class II antigen presentation. Finally, up-regulation of interferon receptor activity and Jak/Stat signaling reached statistical significance in both tissues cited above as well as in the adult Ts1Cje hippocampus (Table III).

Quantitative Real-Time PCR Confirmation of Candidate Genes

To confirm microarray data, we used quantitative real-time PCR amplification to investigate gene expression differences of several genes, including *Dyrk1A* and *Rcan1* (NFAT signaling), *Cyb5r1* (oxidative stress), *Cdc25*, and *Tsga10* (neurogenesis and cell cycle regulation) and *Slc6A9* (SLC-mediated amino acid transport) in E15 brain hemispheres from Ts1Cje (n–= 12) and WT (n = 10) embryos. *Dyrk1A* and *Rcan1* genes were up-regulated in a gene-dosage dependent manner in Ts1Cje (1.43 ± 0.09 and 1.52 ± 0.09) versus WT littermates (1.00 ± 0.06 and 1.00 ± 0.03) ($P = 0.05$, Mann–Whitney test) (Figure SI). The oxidative stress associated gene *Cyb5r1* was also significantly up-regulated in the Ts1Cje embryonic brains (1.58 ± 0.14) compared to their WT littermates

TABLE I. Differentially Expressed Genes in Ts1Cje Embryonic Day 15.5 Brain Versus WT at BH-FDR < 20%

Gene Name and Symbol	Chromosome	Ratio Ts1Cje/WT	Gene Copies
Phosphoribosylglycinamide formyltransferase (*Gart*)	16	1.36	3
Regulator of calcineurin 1 (*Rcan1*)	16	1.29	3
Synaptojanin 1 (*Synj1*)	16	1.30	3
Dual-specificity tyrosine-(Y)-phosphorylation regulated kinase 1A (*Dyrk1A*)	16	1.19	3
RIKEN cDNA 1110004E09 gene (*1110004E09Rik*)	16	1.35	3
Dopey family member 2 (*Dopey2*)	16	1.34	3
Intersectin 1 (SH3 domain protein 1A) (*Itsn1*)	16	1.32	3
Hormonally upregulated Neu-associated kinase (*Hunk*)	16	1.32	3
URB1 ribosome biogenesis 1 homolog (S. cerevisiae) (*Urb1*)	16	1.30	3
Mitochondrial ribosomal protein S6 (*Mrps6*)	16	1.32	3
Interferon gamma receptor 2 (*Ifngr2*)	16	1.29	3
Tryptophan rich basic protein (*Wbr*)	16	1.28	3
Interferon (alpha and beta) receptor 1 (*Ifnar1*)	16	1.36	3
Crystallin, zeta (quinone reductase)-like 1 (*Cryzl1*)	16	1.35	3
Bromodomain and WD repeat domain containing 1 (*Brwd1*)	16	1.43	3
Son DNA binding protein (*Son*)	16	1.39	3
Down syndrome critical region gene 3 (*Dscr3*)	16	1.50	3
Superoxide dismutase 1, soluble (*Sod1*)	16	1.45	3
SR-related CTD-associated factor 4 (*Scaf4*)	16	1.22	3
Transmembrane protein 50B (*Tmem50b*)	16	1.37	3
GC-rich sequence DNA-binding factor 1 (*Gcfc1*)	16	1.39	3
Solute carrier family 5 (inositol transporters), member 3 (*Slc5a3*)	16	1.39	3
Proteasome (prosome, macropain) assembly chaperone 1 (*Psmg1*)	16	1.45	3
Chloride intracellular channel 6 (*Clic6*)	16	1.24	3
Holocarboxylase synthetase (biotin- [propriony-Coenzyme A-carboxylase (ATP-hydrolysing)] ligase) (*Hlcs*)	16	1.23	3
MIS18 kinetochore protein homolog A (S. pombe) (*Mis18a*)	16	1.35	3
Carbonyl reductase 1 (*Cbr1*)	16	1.34	3
DnaJ (Hsp40) homolog, subfamily C, member 28 (*Dnajc28*)	16	1.27	3
Microrchidia 3 (*Morc3*)	16	1.36	3
ATP synthase, H+ transporting, mitochondrial F1 complex, O subunit (*Atp5o*)	16	1.36	3
C2 calcium-dependent domain containing 2 (*C2cd2*)	16	1.32	3
Interferon (alpha and beta) receptor 2 (*Ifnar2*)	16	1.32	3
Downstream neighbor of SON (*Donson*)	16	1.40	3
SET domain containing 4 (*Setd4*)	16	1.13	3
PR domain containing 15 (*Prdm15*)	16	1.21	3
Phosphatidylinositol glycan anchor biosynthesis, class P (*Pigp*)	16	1.23	3
Tetratricopeptide repeat domain 3 (*Ttc3*)	16	1.21	3
Family with sequence similarity 165, member B (*Fam165b*)	16	1.14	3
Zinc finger protein 295 (*Zfp295*)	16	1.17	3
Dynein, axonemal, heavy chain 11 (*Dnahc11*)	12	9.34	1
Integrin beta 8 (*Itgb8*)	12	0.63	1
Trans-acting transcription factor 4 (*Sp4*)	12	0.78	1
Trans-acting transcription factor 8 (*Sp8*)	12	0.78	1
Cytochrome b5 reductase 1 (*Cyb5r1*)	1	1.15	2
Testis specific 10 (*Tsga10*)	1	1.27	2
Cysteine conjugate-beta lyase 1 (*Ccbl1*)	2	1.09	2
Low density lipoprotein receptor-related protein 4 (*Lrp4*)	2	1.08	2
ATPase, class I, type 8B, member 2 (*Atp8b2*)	3	1.10	2
CDC-like kinase 2 (*Clk2*)	3	1.04	2
Regulatory factor X, 5 (influences HLA class II expression) (*Rfx5*)	3	0.80	2
Signal peptide peptidase 3 (*Sppl3*)	5	0.96	2
Zinc finger protein 326 (*Zfp326*)	5	1.10	2
Caprin family member 2 (*Caprin2*)	6	1.14	2
Echinoderm microtubule associated protein like 2 (*Eml2*)	7	1.05	2
STAR-related lipid transfer domain containing 5 (*Stard5*)	7	1.11	2
RIKEN cDNA 1810020D17 gene (*1810020D17Rik*)	7	1.14	2

(*Continued*)

TABLE I. (*Continued*)

Gene Name and Symbol	Chromosome	Ratio Ts1Cje/WT	Gene Copies
B cell translocation gene 4 (*Btg4*)	9	1.06	2
DENN/MADD domain containing 4A (*Dennd4a*)	9	1.10	2
Transmembrane protein 42 (*Tmem42*)	9	1.17	2
Ubiquitin specific peptidase 28 (*Usp28*)	9	1.10	2
Vacuolar protein sorting 13C (yeast) (*Vps13c*)	9	1.16	2
Transducin-like enhancer of split 2, homolog of Drosophila E(spl) (*Tle2*)	10	0.96	2
Protein phosphatase 4, regulatory subunit 4 (*Ppp4r4*)	12	1.16	2
RIKEN cDNA 4930447C04 gene (*4930447C04Rik*)	12	1.44	2
Thiopurine methyltransferase (*Tpmt*)	13	1.32	2
ER membrane protein complex subunit 2 (*Emc2*)	15	1.13	2
PRP40 pre-mRNA processing factor 40 homolog B (yeast) (*Prpf40b*)	15	1.08	2
DnaJ (Hsp40) homolog, subfamily C, member 4 (*Dnajc4*)	19	1.20	2
Pellino 3 (*Peli3*)	19	1.05	2
cDNA sequence BC022960 (*BC022960*)	X	1.26	2
Histone deacetylase 6 (*Hdac6*)	X	1.18	2

(1.00 ± 0.06) ($P = 0.01$, Mann–Whitney test) (Figure SI). Similar to the microarray data, cell cycle and neurogenesis genes *Cdc25* and *Tsga10* were also up-regulated in the Ts1Cje embryonic brain (1.23 ± 0.14 and 1.24 ± 0.09) versus WT littermates (1.00 ± 0.11 and 1.00 ± 0.13). This up-regulation, however, did not reach statistical significance (Figure SI). Finally, *Slc6A9* gene expression was down-regulated in Ts1Cje embryonic brain hemispheres (0.75 ± 0.08) versus WT littermates (1.00 ± 0.18) in agreement with the microarray data (Figure SI).

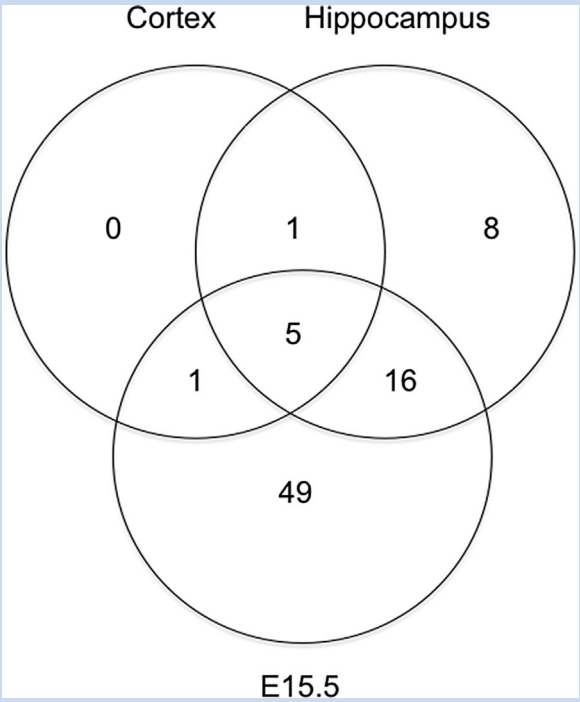

FIG. 1. Venn diagram representing the number of differentially regulated genes in the Ts1Cje embryonic day 15.5 (E15.5) brain versus adult cerebral cortex and hippocampus at BH-FDR<20%. Ts1Cje E15.5 brains display more differentially regulated genes (71 genes) compared to the adult cortex (7 genes) and hippocampus (30 genes) when compared to their respective littermate controls. Five genes (*Gart*, *Rcan1*, *Synj1*, *Dyrk1A*, and *Dnahc11*) were consistently up-regulated in all tissues examined.

Developmental Milestones and Neonatal Behavior in Ts1Cje Mice

Delay of developmental milestones in Ts1Cje mice. Analysis of growth profiles of the Ts1Cje pups and their control littermates between P3 and P21 revealed that the former demonstrated significant growth delays throughout the first month of life. Total body weight was 17–30% lower at all time points in Ts1Cje (median = 4.54 g, sum of ranks = 94.24) versus WT pups (median=6.34 g, sum of ranks = 127.8) ($P < 0.0001$, Wilcoxon signed-rank test) (Fig. 3A). Paired analyses also showed that total body and tail base lengths were significantly smaller in the Ts1Cje animals ($P < 0.0001$, Mann–Whitney test) (Fig. 3B). For the biometry (body weight, tail base length, and total length), values passed the normality test at all postnatal days and the variances were equal. Both non-parametric and parametric tests yielded similar results (Data not shown).

The growth delays in Ts1Cje mice were also associated with early neonatal behavioral deficits. For developmental milestones statistics, even though the two populations passed the normality test for a few postnatal days, it did not for others. Thus, we have used non-parametric Mann–Whitney and Wilcoxon signed-rank tests. A significant delay in acquiring several developmental milestone was observed for Ts1Cje compared to their WT littermates. Even after acquiring these milestones, Ts1Cje neonates had significantly lower performance versus WT. After several days of testing, Ts1Cje neonates were able to catch-up with their WT littermates for most milestones between days P11 and P14 (Fig. 3C–F, Table IV). Analysis of body righting and coordination tests showed that Ts1Cje neonates had a significantly higher latency in the surface righting (median = 16.93 sec, sum of ranks = 171.8) and negative geotaxis (median = 20.87 sec, sum of ranks = 224.2) tests

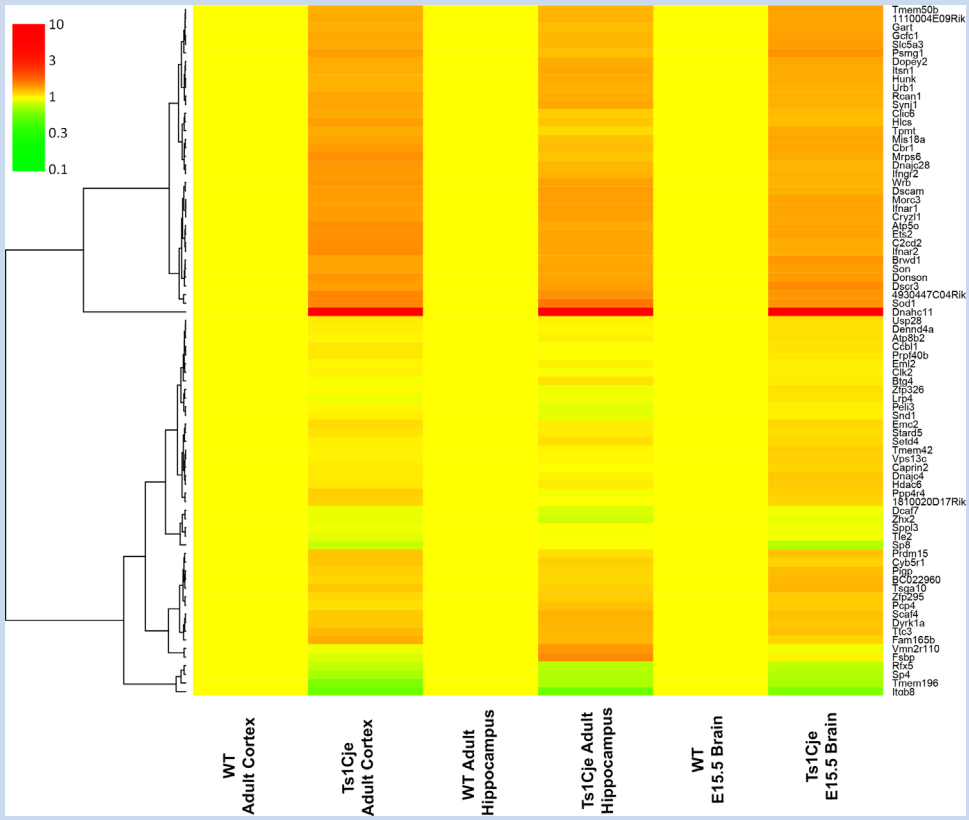

FIG. 2. Heatmap for the Ts1Cje embryonic day 15.5 (E15.5) brain, adult cerebral cortex and adult hippocampus. Differentially expressed genes at BH-FDR<20% are indicated on the right side of the graph. Regulation direction of differentially expressed genes is highly correlated in the three tissues examined, particularly between the embryonic E15.5 brain and adult cerebral cortex. Gene expression regulation in Ts1Cje is indicated in red (up-regulation), yellow (no change) and green (down-regulation) compared to wild-type embryos. WT: wild type.

than WT neonates (median = 5.71 sec, sum of ranks = 130 and median = 14.19 sec, sum of ranks = 184.9, respectively) ($P = 0.001$, Wilcoxon signed-rank test) (Fig. 3C–D). We combined these tests with the cliff aversion and forelimb grasp paradigms to grossly examine body strength in the Ts1Cje pups. The results revealed significantly decreased body strength in Ts1Cje neonates (median = 15.17 sec, sum of ranks = 177.3 and median = 3.30 sec, sum of ranks = 30.88 for cliff aversion and forelimb grasp, respectively) versus their WT littermates (median = 7.02 sec, sum of ranks = 112.3 and median = 5.01 sec, sum of ranks = 46.5, respectively) ($P < 0.001$, Wilcoxon signed-rank test) (Fig. 3E–F). Paired analyses of Ts1Cje performance on every postnatal day highlighted significant deficits in most of these tests between days P5 and P10 ($P < 0.05$–0.0001, Mann–Whitney test). In contrast, however, there were no differences between Ts1Cje (median = 23.79 sec, sum of ranks = 387.5) and WT pups (median = 24.44 sec, sum of ranks = 371.9) in the open field test. It is important to point out the fact that for the days that passed the normality test, a parametric t-test was performed and yielded similar results (Data not shown).

Sex-specific differences in developmental milestones of Ts1Cje mice. At postnatal day 3, both Ts1Cje females (n = 12) and males (n = 17) showed similar reductions in body weight (−16 and −14%) and total body length (−6%) when compared to their littermate WT pups (n = 25 males and 39 females). In Ts1Cje males, this difference increased to 31% at P5 then 35% at P10 before stabilizing at 30% between days P15 and P21. In the Ts1Cje females, weight reduction reached 25–30% between P5 to P10 before decreasing to 19% at P15 and 16% at P21 (Figure SII). However, both Ts1Cje males and females showed similar total body length reduction (6–7% at P3, 11% at P10 and 10–12% at P13).

Analysis of the postnatal day at which Ts1Cje males and females achieved different developmental milestones revealed that surface righting and cliff aversion were more severely affected in males (9.31 ± 2.17 and 9.57 ± 2.38 days) versus females (8.54 ± 1.37 and 7.82 ± 2.14 days) when compared to WT males (7.92 ± 1.38 and 6.54 ± 1.84 days) and females (7.81 ± 1.20 and 6.15 ± 1.60 days) for surface righting and cliff aversion, respectively (Table SIII, Figures SII–III). In the negative geotaxis test, Ts1Cje males (9.31 ± 2.29 days) performed better than their female counterparts (9.82 ± 2.31 days) versus WT males (8.22 ± 1.73 days) and females (7.66 ± 2.33 days) (Table SIII, Figures SIII). No sex-specific differences were found in the other developmental milestones, and both Ts1Cje males and females were delayed compared to their WT sex-matched littermates (Table SIII, Figures SIII–V). Detailed

TABLE II. DAVID Analysis Results for the E15.5 Embryonic Brain in Ts1Cje Mice

Enriched Functional Categories	Counts*	DAVID *P*-value	Fold Enrichment	Direction	Example of Regulated Genes
Cell cycle GO:0007049	30	1.50E-11	4.47	UP	*Ccnb2, Aurkb, Cdc2a, Cdk1, Kif18a, Cdk6, Zwilch, Nusap1, Bub1, Kif4, Cenpe, Cenpf*
Phosphorus metabolic process GO:0006793	17	0.021	1.84	UP	*Cdk1, Pnck, Plk1, Dyrk1A, Melk, Aurkb*
Purine nucleotide binding GO:0017076	30	0.007	1.62	UP	*Coasy, Hlcs, Acss2, Ddx3Y, Top2a*
Cytoskeleton GO:0005856	18	0.025	1.74	UP	*Dlgap5, Kif15, Cenpf, Nusap1, Calcoco2*
Interferon activity receptor GO:0004904	2	0.02	101.4	UP	*Ifnar1, Ifnar2*
Neurological system process GO:0050877	29	0.004	−1.71	DOWN	*Olfr331, Agt, Dlgap1, Aars, Tbx1, Penk*
Cell surface receptor linked signaling transduction GO:0007166	30	0.01	−1.58	DOWN	*Gpr84, Olfr539, Eif4ebp1, Vnmr2R60, Nmbr*
Sensory perception GO:0007600	25	0.006	−1.77	DOWN	*Olfr135, Olfr331, Olfr151, Olfr488, Olfr559*
MHC class I protein complex GO:0042611	4	0.015	−7.53	DOWN	*H2-M1, H2-Q9, C920025e04rik, Gm10499*
Translation GO:0006412	10	0.005	−3.11	DOWN	*Iars, Tars, Cars, Nars, Rpl29*
Amine transmembrane transporter activity GO:0005275	7	2.69E-05	−11.72	DOWN	*Slc1a4, Slc6a9, Slc7a3, Slc6a4, Slc25a18, Slc3a2, Slc7a5*
Oxidoreductase activity, acting on the CH-NH group of donors, NAD or NADP as acceptor GO:0016646	3	0.008	−21.09	DOWN	*Mthfd2, Pycr1, Aldh1l2*
Cell adhesion GO:0007155	14	0.004	−2.46	DOWN	*Pcdhga10, Igfbp7, Vwf, Cdh9*

*The number of up- and down-regulated genes among the counts, the corresponding DAVID P-values, fold enrichment and direction of regulation are indicated.

examination of longitudinal performances during the entire testing period confirmed that Ts1Cje males demonstrated more significant deficits than the Ts1Cje females during more postnatal dates in the surface righting, negative geotaxis and cliff aversion tests. No differences were noticed in the forelimb grasp and open field tests (Table SIV, Figures SIII–V).

Ultrasonic vocalization pattern in Ts1Cje neonates. Ts1Cje neonates produced significantly more USVs in the screening trial (5.15 ± 1.64 USVs, sum of ranks = 274.5) when compared to WT pups (0.89 ± 0.66 USVs, sum of ranks = 221.5) ($P = 0.001$, Mann–Whitney test) (Fig. 4A). No significant differences, however, were observed in the testing trial ($P = 0.32$, Mann–Whitney test) (Fig. 4B). Ts1Cje exhibited a significant reduction of motor activity (12.92 ± 3.12 crossings, sum of ranks = 141.5) versus WT littermates (32.22 ± 6.15 crossings, sum of ranks = 354.5) ($P < 0.01$, Mann–Whitney test) (Fig. 4C). No differences were observed in the number of body rolls in both groups ($P = 0.43$, Mann–Whitney test) (Fig. 4D). Both screening and testing did not pass normality test, however, grid crossing and body rolls did and yielded similar results with parametric t-test (Data not shown).

Olfactory spatial memory in Ts1Cje neonates. In the homing test, two Ts1Cje (17%) and 12 WT (75%) pups were able to reach the goal area in trial 1 and/or trial 2. Ts1Cje pups displayed a significant olfactory spatial memory deficit manifested by a significant increase in the amount of time needed to reach the goal area in trial 1 (166.0 ± 31.8 sec, sum of ranks = 224.0) compared to their WT littermates (113.1 ± 64.5 sec, sum of ranks = 182.0) ($P < 0.01$, Mann–Whitney test) (Fig. 5A). In trial 2, WT pups showed decreased latency to reach the goal area (89.3 ± 67.4 sec, sum of ranks = 176.5) than in trial 1 (113.1 ± 64.5 sec, sum of ranks = 182.0) but this reduction was not statistically significant. However, Ts1Cje performed equally poorly in both trials (166.0 ± 31.8 sec in trial 1 versus 167.7 ± 42.7 sec in trial 2) (Fig. 5A). We did not observe any major motor deficits in the Ts1Cje at P12 that could have led to their poor performance in the homing test (Fig. 5B).

DISCUSSION

In the present study, we demonstrated that significant gene expression abnormalities were already present in the embryonic day 15.5 brain hemispheres of the Ts1Cje mouse model of DS when compared with euploid controls. In addition, Ts1Cje neonates displayed early postnatal developmental milestone delays and behavioral changes during the pre-weaning period.

Significant Molecular Changes Are Present in Ts1Cje Embryonic Brains

At a BH-FDR≤20% cut-off, 71 genes were significantly differentially regulated in the Ts1Cje E15.5 embryonic brain compared to age and sex-matched controls, indicating that significant molecular perturbations are already present during fetal brain development in the Ts1Cje model. In contrast with the adult brain, in which most differentially regulated genes were present in three copies, more diploid genes were dysregulated in the Ts1Cje embryonic brain, suggesting a larger genome-wide secondary effect during fetal development.

Similar changes were observed during early postnatal cerebellum development in the Ts1Cje mice versus their euploid litter-

TABLE III. List of Up-and Down-Regulated Gene Sets in the Embryonic Ts1Cje Brain Gene Expression Data Identified With Gene Set Enrichment Analysis (GSEA)

GSEA Gene Set	Gene Set Collection	NES E15.5 Brains	*P* Value E15.5 Brains	Regulation in Adult CRTX	Regulation in Adult HIP
Up-regulated pathways in E15.5 Ts1Cje brains					
CHR21Q21-22	C1	3.12	0	UP	UP
Reactome-cell cycle	C2	2.15	0	UP	Unchanged
M-G1 phases	C2	2.04	0.0018		
G1-S phases	C2	1.62	0.039		
Cell cycle	C5	1.87	0		
Reactome-apoptosis	C2	1.51	0.04	UP	UP
Apoptotic execution phase	C2	1.60	0.02		
Apoptotic program	C5	1.54	0.04		
Reactome MHC class II antigen presentation	C2	1.52	0.047	UP	Unchanged
Cytokine binding	C5	1.44	0.049		
Kinase activity	C5	1.53	0.017	UP	Unchanged
Protein Ser/Thr kinase activity		1.80	0.01		
Cytoskeleton	C5	1.52	0.022	Unchanged	Unchanged
ATPase activity	C5	1.54	0.042	Unchanged	Unchanged
JAK/STAT cascade	C5	1.71	0.017	UP	UP
Down-regulated pathways in E15.5 Ts1Cje brains					
Behavior	C5	−1.38	0.034	DOWN	DOWN
Reactome-GPRC down-stream signaling	C2	−1.41	0.034	DOWN	DOWN
G-protein coupled receptor protein signaling	C5	−1.80	0.002		
Reactome-Neuronal system	C2	−1.62	0.026	DOWN	DOWN
Synaptic transmission	C5	−1.65	0.015		
Reactome-SLC mediated transmembrane transport	C2	−1.47	0.033	DOWN	Unchanged
Amino acid transport	C5	−1.98	0.002		
Reactome-Potassium channels	C2	−1.62	0.026	DOWN	DOWN
Reactome-GABAR activation	C2	−1.61	0.013		
Glutamate receptor activity	C5	−1.73	0.017		
Reactome-Chemokine receptors bind chemokines	C2	−1.73	0.016	Unchanged	Unchanged
Chemokine activity	C5	−1.51	0.033		
Reactome-Glycosphingolipid metabolism	C2	−1.47	0.047	Unchanged	Unchanged
Phosphoinositide mediated signaling	C5	−1.45	0.045		
Reactome-Transferrin endocytosis and recycling	C2	−1.62	0.031	Unchanged	Unchanged
Insulin receptor recycling	C2	−1.55	0.045		

Table includes NESs (normalized enrichment scores) and *P*-values as reported by GSEA. The most significantly enriched sets are indicated. CRTX: Cerebral cortex; HIP: Hippocampus. Data from adult Ts1Cje cerebral cortex and hippocampus are from Guedj et al., 2015.

mates. Indeed, more differentially regulated genes (419 genes) were observed at birth (postnatal day 0) compared to P15 (339 genes) and P30 (257 genes) cerebella using a raw *P* value of 0.01 as cut-off [Potier et al., 2006].

Unfortunately, there are very little published data on how gene expression is modified in the human fetal brain compared to the adult brain in Down syndrome. Lockstone et al. (2007) reported 685 differentially regulated genes in seven adult post-mortem human brains with DS versus eight euploid matched controls. The same authors re-analysed the DS fetal brain dataset generated by Mao et al. (2005) and found only 21 differentially regulated genes during the second trimester. This limited number of regulated genes is probably the result of the small sample size (n = 4 per karyotype) used in the study, suggesting that more human data are needed to establish a clear picture on how gene expression is modified in the fetal and adult DS brain.

Pro-Cell Cycle Markers Are Highly Enriched in Ts1Cje Fetal Brain

To circumvent the low number of differentially regulated genes and be able to identify molecular pathways or cellular processes that are significantly dysregulated in Ts1Cje fetal brain, we performed functional analysis via GSEA and DAVID databases on the top 1% up- and down-regulated genes.

Unexpectedly, pro-cell cycle markers that play a key role in mitosis regulation were highly enriched in the Ts1Cje embryonic brain. These genes belong to two categories: (1) Cyclins/cyclin-dependent

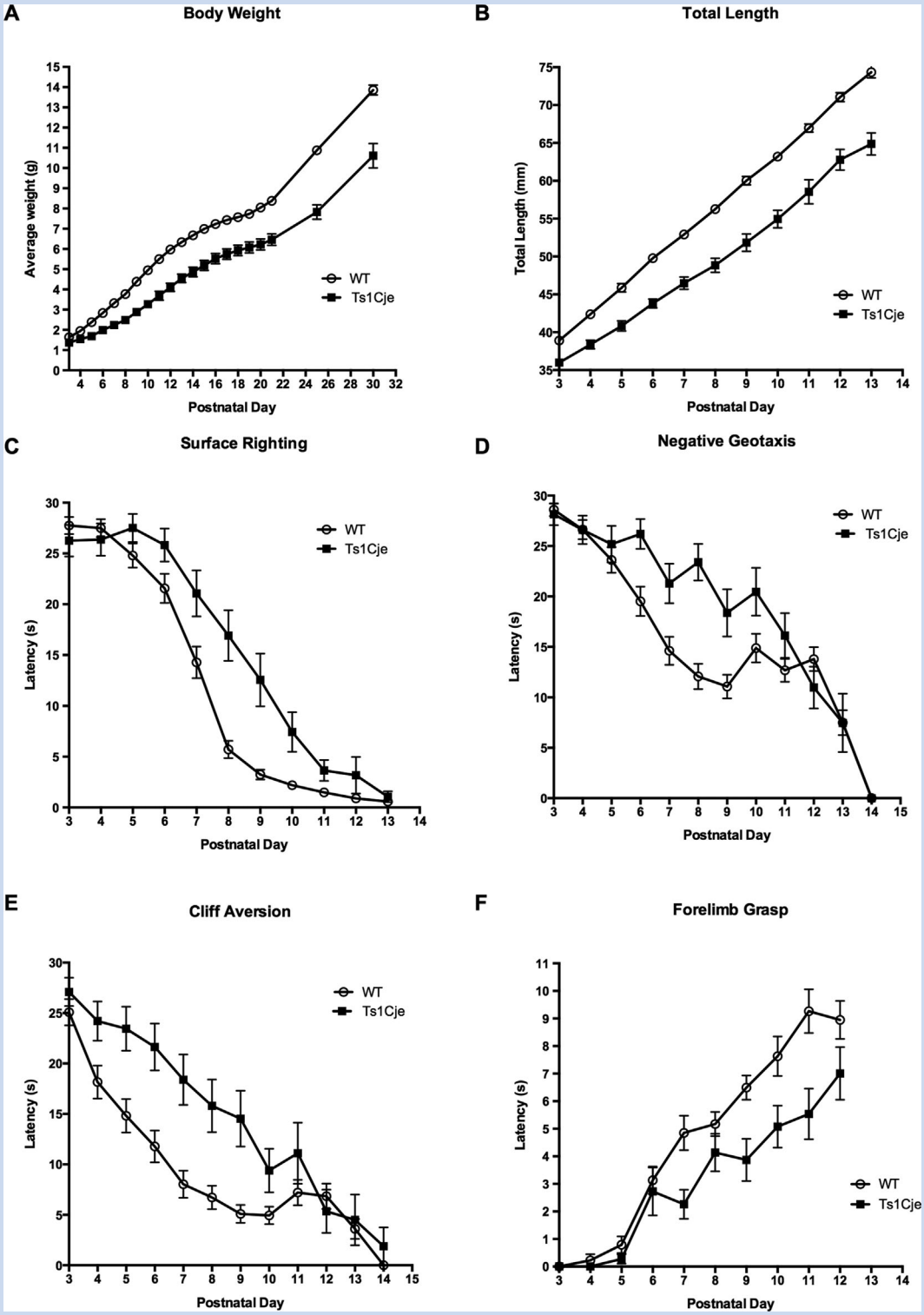

FIG. 3. Growth Profile and Developmental Milestones in the Ts1Cje Mouse Model During the Pre-Weaning Period. A–B: Total body weight was measured on a daily basis between postnatal days 3 and 21 (A), and total length was assessed before eye opening (B) in Ts1Cje pups ($n = 29$) and their littermate wild-type pups ($n = 64$). Trisomic pups display a marked growth delay during the first month after birth. C–F: Developmental milestones were analyzed using a modified Fox scale to assess body righting, coordination and strength via the surface righting (C), negative geotaxis (D), cliff aversion (E) and forelimb grasp (F) tests between postnatal day 3 and 14 (i.e., Before eye opening). Ts1Cje neonates show a marked delay in acquiring all these milestones compared to WT pups. Data are represented as mean $\pm$ SEM. WT: Wild type.

TABLE IV. Average Postnatal Day at Which Development Milestone Is Achieved

Developmental Milestone	WT (n = 64) postnatal day ± SD	Ts1Cje (n = 29) postnatal day ± SD
Body righting and coordination		
Surface righting	7.87 ± 1.23	8.69 ± 1.23*
Negative geotaxis	7.82 ± 2.03	9.30 ± 2.41*
Air righting	14.93 ± 1.31	16.62 ± 1.45*
Strength		
Cliff aversion	6.30 ± 1.64	8.60 ± 2.34*
Forelimb grasp	7.50 ± 1.13	8.20 ± 1.58*
Sensory system maturation		
Eye opening	13.97 ± 0.88	14.75 ± 1.34
Ear opening	5.38 ± 0.81	5.96 ± 0.93
Ear twitch	14.23 ± 1.15	15.5 ± 1.46*
Auditory startle	14.20 ± 1.11	15.37 ± 1.26
Extinction of rotatory behavior		
Open field	13.46 ± 2.53	13.75 ± 2.95

List of neonatal behavioral tests included in the Fox scale. Data presented in this table represent the postnatal day at which the pups performed successfully the tests for two consecutive days. Tests for which the Ts1Cje pups displayed a statistically significant delay are indicated with an asterisk. WT: Wild Type.

kinases coding genes (e.g., *Cdk1*, *Cdc25c*, *Ccnb2*, *Cdca2*, and *Cdca3*) and (2) Bipolar spindle and kinetochore complex coding genes (e.g., *Kif11*, *Kif18a*, *Cenpe*, and *Bub1*). Expression of these genes is tightly regulated through very complex mechanisms and their gene dosage alteration is associated with developmental defects and cancer [Rieder and Salmon, 1998; Stewart et al., 2003; Santamaria and Ortega, 2006].

Several genes identified in our dataset, including *Cdk1*, *Cenpf*, *Nusap1*, *Aurkb*, and *Tacc3* play a crucial role in brain development and function, and their dysregulation is associated with neurodevelopmental or neurodegenerative conditions [Camargo et al., 2007; Schick et al., 2007; Nie et al., 2010; Marchal et al., 2011; Yang et al., 2012; Satoh et al., 2013].

Multiple studies have reported decreased neurogenesis in human fetuses with Down syndrome and different mouse models (Ts65Dn, Ts1Cje, and Ts2Cje) but no molecular mechanisms were provided to understand the origin of the phenotypic differences [Schmidt-Sidor et al., 1990; Chakrabarti et al., 2007; Ishihara et al., 2010; Guidi et al., 2011]. A plausible explanation for this apparent contradiction might be that Ts1Cje embryonic brains display prolonged cell cycle duration that results in increased gene expression of pro-cell cycle genes, but a reduced cell proliferation rate. In line with this hypothesis, using bromodeoxyuridine (BrdU) staining, analysis of Ts65Dn embryonic brains and cultured Ts1Cje neurospheres revealed a significant increase in cell cycle duration [Chakrabarti et al., 2007; Moldrich et al., 2009; Ishihara et al., 2010].

We hypothesize that this cell cycle delay is triggered by the activation of a cellular repair mechanism during the metaphase-anaphase transition in an attempt to correct the aneuploidy after the alignment of sister chromatids in the bipolar spindle. In the Ts1Cje mice, the cell detects a misalignment of the sister spindle microtubule-kinetochore complexes containing the normal MMU12 and the translocated MMU12[16]. This potentially sends an alarm signal that activates the mitotic checkpoint complex and arrests the cell cycle during the M-phase to initiate the cell repair mechanism. The mitotic checkpoint complex (MCC) consists of BubR1, Bub1, Bub3, Cdc20, and Mad1 proteins, and interacts with several other kinetochore proteins, including Cenpe, Cenpf, Sgol2, Aurkb, and Kif18a to regulate the metaphase-anaphase transition [Chan et al., 2005; Huang et al., 2007; Sczaniecka and Hardwick, 2008]. In the present study, we observed an up-regulation of most of these genes (*BubR1*, *Bub1*, *Cenpe*, *Cenpf*, *Sgol2*, *Aurkb*, and *Kif18a*) in the Ts1Cje embryonic brain, supporting our hypothesis. Moreover, Bhattacharyya et al [Bhattacharyya et al., 2009] reported up-regulation of several genes encoding the MCC complex and regulating the metaphase-anaphase transition (*Aurkb*, *Cenpe*, *Cenpf*, *Apc*, *Ctnnbip1*) in human neural progenitor cells (hNPCs) derived from cortex of 13-week gestation fetuses with DS. This suggests that the findings obtained in mouse models [Chan et al., 2005; Chakrabarti et al., 2007; Moldrich et al., 2009; Ishihara et al., 2010] can shed light on the human etiology of DS.

Amino-Acid Mediated Neurotransmitter Transport is Down-Regulated in Ts1Cje Fetal Brain

Ts1Cje embryonic brains display a significant down-regulation of several SLC solute carrier coding genes known to play a key role in serotonin, NMDA and L-DOPA transmembrane transport, including *Slc6a4*, *Slc25a18*, *Slc1a4*, *Slc6a9*, *Slc7a3*, *Slc3a2*, and *Slc7a5*.

Solute carrier proteins represent the largest group of membrane transporters with more than 384 unique protein sequences from 52 distinct SLC families that regulate the transport of a wide variety of substrates, such as neurotransmitters, inorganic ions, nucleotides, sugars, purine, fatty acids and drug molecules. There is a growing interest in the use of these transporters as therapeutic targets for several mental conditions, including epilepsy, depression and addiction [Girardin, 2006; Rask-Andersen et al., 2013].

Slc6a4 (Serotonin reuptake transporter or Sert), which is up-regulated in the Ts1Cje embryonic brain, has been targeted by

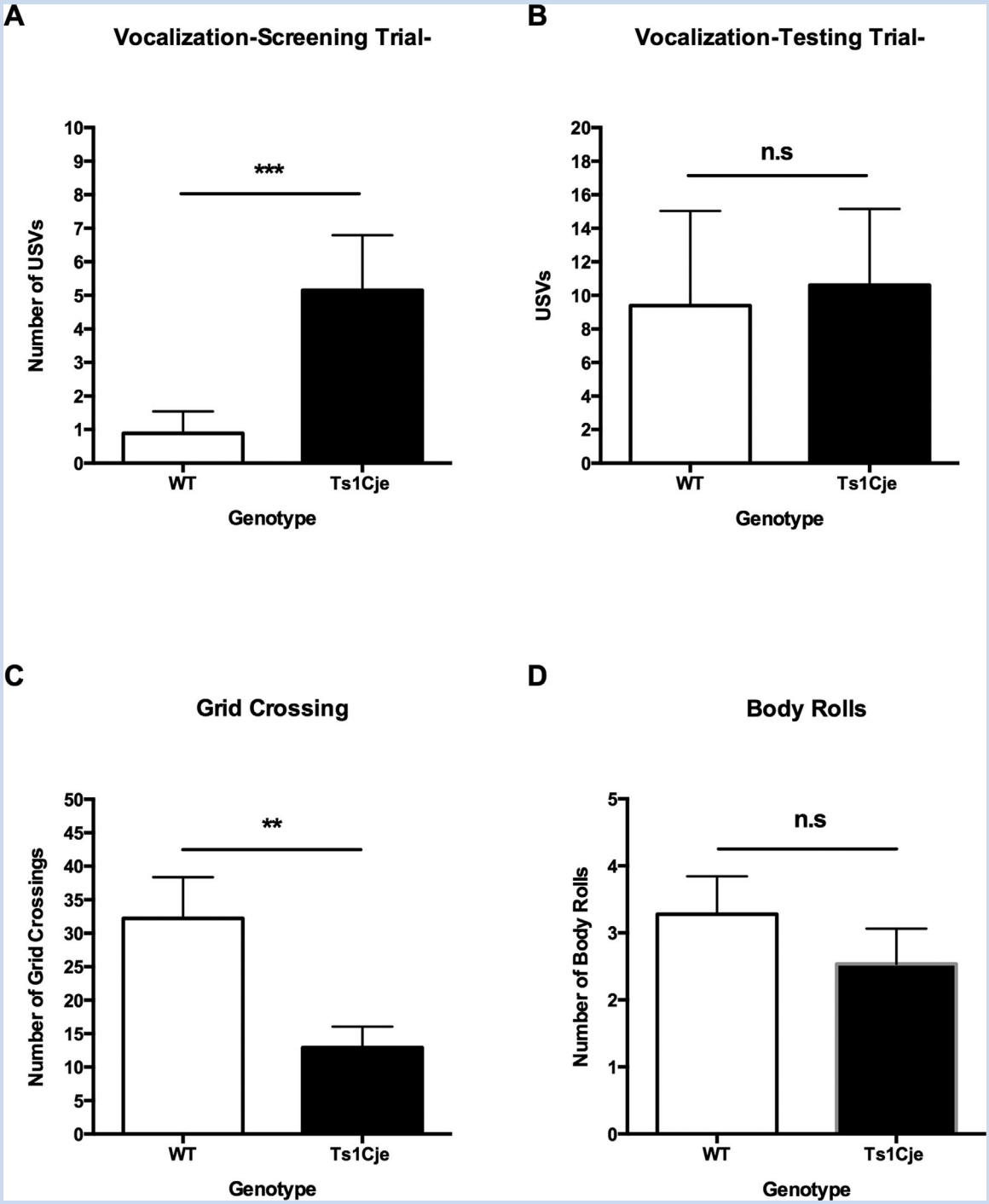

FIG. 4. Ultrasonic Vocalization and Motor Activity in the Ts1Cje Mouse Model During the Pre-Weaning Period. A–B: Ts1Cje pups (n = 13) produce more ultrasonic vocalization during the screening trial (A) versus wild-type pups (n = 18), but not during the testing trial (B). C–D: Ts1Cje pups show reduced number of grid crossings (motor activity) but not body rolls compared to WT neonates during the testing trial. Data are represented as mean ± SEM. WT: Wild type.

drugs such as fluoxetine to inhibit serotonin reuptake as a treatment for depression [Andersen et al., 2014]. Prenatal and early postnatal treatment with fluoxetine results in a long lasting positive impact on brain development (neurogenesis and synaptogenesis) and behavior in the Ts65Dn mouse model of DS [Bianchi et al., 2010; Guidi et al., 2013; Guidi et al., 2014]. This therapeutic effect might be mediated through the inhibition of *Slc6a4* mediated serotonin reuptake.

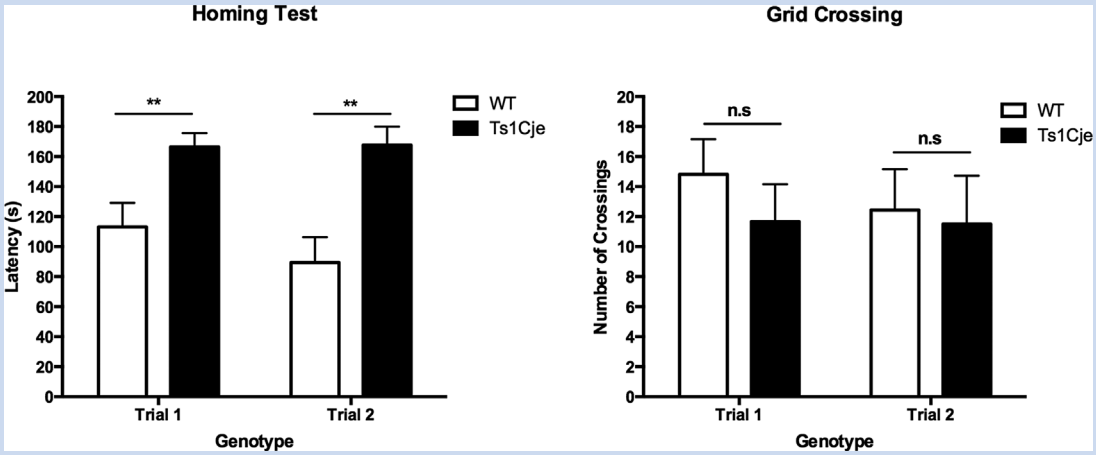

FIG. 5. Olfactory Spatial Memory in the Ts1Cje Mouse Model During the Pre-Weaning Period. A: Ts1Cje pups (n = 12) have a longer latency to reach the homing test goal area in both trial one and two compared to their littermate WT controls (n = 16). B: The number of grid crossings was not significantly affected in the Ts1Cje at P12, indicating that their poor performance in the homing test was not the result of motor deficits. Data are represented as mean ± SEM. WT: Wild type.

Slc6a9 (*Glyt1*), which is up-regulated in Ts1Cje E15.5 brains, is highly expressed in the brain during embryonic development. Its targeted disruption is linked to severe sensorimotor deficits and early postnatal lethality in mice [Jursky and Nelson, 1996; Bakkar et al., 2011]. *Slc6a9* plays a role in the regulation of glycine levels in NMDA receptor-mediated neurotransmission, and is used as a therapeutic target for schizophrenia [Bergeron et al., 1998; Mohler et al., 2011]. In vitro and in vivo modulation of *Slc6a9* expression is associated with NMDA neurotransmission facilitation and working memory enhancement [Yee et al., 2006; Singer et al., 2009].

Another interesting SLC-transporter up-regulated in the Ts1Cje E15.5 brains is *Slc7a5* (*Lat1*) involved in the transport of L-DOPA through the blood brain barrier as well as the transport of thyroid hormones T3 and T4 across the cell membrane [Bik-Multanowski and Pietrzyk, 2006; Braun et al., 2011; Chan et al., 2011]. Hypothyroidism is a common clinical problem in children with Down syndrome that may also affect their neurocognitive development [Purdy et al., 2014; Van Trotsenburg et al., 2003].

Significant Behavioral Abnormalities Are Present in Ts1Cje Neonates

We combined a systems biology approach with behavioral testing to establish a comprehensive catalog of the prenatal and early postnatal phenotype in the Ts1Cje mouse model of DS. Our approach revealed that both fetal brain pathway dysregulation and neonatal behavioral deficits are present in this model.

Functional pathway analyses showed that a number of neurological systems processes (i.e., cognition and behavior) were altered in the Ts1Cje embryonic brain. These molecular changes were accompanied by significant postnatal delays in acquiring different developmental milestones, including body righting, coordination, strength, and sensory maturation in this model. Furthermore, even after acquiring these skills, Ts1Cje pups showed increased delay in performing these tests versus their wild-type littermates. In the ultrasonic vocalization test, trisomic pups uttered more vocalizations when subjected to external stress, indicating increased anxiety, and delayed pattern of vocalization in the Ts1Cje animals. This increased anxiety was associated with reduced motor activity.

G-protein signaling, most importantly olfactory receptor activity, was also down-regulated in the Ts1Cje embryonic and adult brains. To get insights into the phenotypic consequences of such changes, we investigated olfactory spatial memory in Ts1Cje neonates and recorded very poor performances of trisomic pups versus WT in the homing test. Our results suggest a strong relationship between embryonic gene expression dysregulation and neonatal development and behavior deficits in the Ts1Cje mouse model of DS.

In the Ts65Dn model, Holtzman et al. (1996) reported comparable milestones and spatial olfactory memory deficits as well as delayed pattern of vocalization in the period between birth and weaning. The molecular origins underlying these behavioral deficits were not investigated. Our results help to uncover some of the signaling pathways that can contribute to these deficits.

CONCLUSIONS

In this study, we used a novel integrated approach that combined gene expression microarray studies and neonatal behavioral testing to provide a comprehensive early phenotype of the Ts1Cje mouse model of Down syndrome. This approach identified several pathway and behavioral abnormalities during critical periods of fetal and neonatal development. These baseline differences can be used to design and evaluate future prenatal therapeutic strategies to improve brain development and cognitive outcome in human fetuses and infants with Down syndrome.

ACKNOWLEDGMENTS

This work was supported by a sponsored research grant from Verinata Health, Inc., an Illumina company, and the Eunice Kennedy Shriver National Institute of Child Health and Human Development grant number R01HD058880-01. The funders had no role in study design, data collection and analysis, decision to publish, or preparation of the manuscript. We would like to thank Dr. Tarik Haydar and Dr. Jose Luis Olmos-Serrano (Laboratory of Neural Development and Intellectual Disorders at Boston University), as well as Tufts Center for Neuroscience Research P30 NS047243 (Dr. Rob Jackson) for their help and suggestions concerning the neonatal behavioral tests. We also acknowledge support from the Hearst Foundations for the purchase of the Quant-Studio Flex 7 quantitative PCR machine.

ACCESSION NUMBERS

The Gene Expression Omnibus (GEO) accession number of the Ts1Cje embryonic day E15.5 brain microarray dataset reported in this paper is GSE62538.

REFERENCES

Amano K, Sago H, Uchikawa C, Suzuki T, Kotliarova SE, Nukina N, Epstein CJ, Yamakawa K. 2004. Dosage-dependent over-expression of genes in the trisomic region of Ts1Cje mouse model for Down syndrome. Hum Mol Genet 13:1333–1340.

Andersen J, Stuhr-Hansen N, Zachariassen LG, Koldso H, Schiott B, Stromgaard K, Kristensen AS. 2014. Molecular basis for selective serotonin reuptake inhibition by the antidepressant agent fluoxetine (prozac). Mol Pharmacol 85:703–714.

Bakkar W, Ma CL, Pabba M, Khacho P, Zhang YL, Muller E, Martina M, Bergeron R. 2011. Chronically saturating levels of endogenous glycine disrupt glutamatergic neurotransmission and enhance synaptogenesis in the CA1 region of mouse hippocampus. Synapse 65:1181–1195.

Bergeron R, Meyer TM, Coyle JT, Greene RW. 1998. Modulation of N-methyl-D-aspartate receptor function by glycine transport. Proc Natl Acad Sci USA 95:15730–15734.

Bik-Multanowski M, Pietrzyk JJ. 2006. LAT1 gene variants-potential factors influencing the clinical course of phenylketonuria. J Inherit Metab Dis 29:684–684.

Braun D, Kinne A, Brauer AU, Sapin R, Klein MO, Kohrle J, Wirth EK, Schweizer U. 2011. Developmental and cell type-specific expression of thyroid hormone transporters in the mouse brain and in primary brain cells. Glia 59:463–471.

Benjamini Y, Hochberg Y. 1995. Controlling the false discovery rate: A practical and powerful approach to multiple testing. J R Stat Soc B 57:289–300.

Bhattacharyya A, McMillan E, Chen SI, Wallace K, Svendsen CN. 2009. A critical period in cortical interneuron neurogenesis in Down syndrome revealed by human neural progenitor cells. Dev Neurosci 31:497–510.

Bianchi P, Ciani E, Guidi S, Trazzi S, Felice D, Grossi G, Fernandez M, Giuliani A, Calza L, Bartesaghi R. 2010. Early pharmacotherapy restores neurogenesis and cognitive performance in the Ts65Dn mouse model for Down syndrome. J Neurosci 30:8769–8779.

Camargo LM, Collura V, Rain JC, Mizuguchi K, Hermjakob H, Kerrien S, Bonnert TP, Whiting PJ, Brandon NJ. 2007. Disrupted in schizophrenia 1 interactome: Evidence for the close connectivity of risk genes and a potential synaptic basis for schizophrenia. Mol Psychiatry 12:74–86.

Chakrabarti L, Galdzicki Z, Haydar TF. 2007. Defects in embryonic neurogenesis and initial synapse formation in the forebrain of the Ts65Dn mouse model of Down syndrome. J Neurosci 27:11483–11495.

Chan GK, Liu ST, Yen TJ. 2005. Kinetochore structure and function. Trends Cell Biol 15:589–598.

Chan SY, Martin-Santos A, Loubiere LS, Gonzalez AM, Stieger B, Logan A, McCabe CJ, Franklyn JA, Kilby MD. 2011. The expression of thyroid hormone transporters in the human fetal cerebral cortex during early development and in N-tera-2 neurodifferentiation. J Physiol 589:2827–2845.

Covington HE 3rd, Miczek KA. 2003. Vocalizations during withdrawal from opiates and cocaine: Possible expressions of affective distress. Eur J Pharmacol 467:1–13.

Dirks A, Fish EW, Kikusui T, van der Gugten J, Groenink L, Olivier B, Miczek KA. 2002. Effects of corticotropin-releasing hormone on distress vocalizations and locomotion in maternally separated mouse pups. Pharmacol Biochem Behav 72:993–999.

Esposito G, Imitola J, Lu J, De Filippis D, Scuderi C, Ganesh VS, Folkerth R, Hecht J, Shin S, Iuvone T, Chesnut J, Steardo L, Sheen V. 2008. Genomic and functional profiling of human Down syndrome neural progenitors implicates S100B and aquaporin 4 in cell injury. Hum Mol Genet 17: 440–457.

Fox WM. 1965. Reflex-ontogeny and behavioural development of the mouse. Anim Behav 13:234–241.

Girardin F. 2006. Membrane transporter proteins: A challenge for CNS drug development. Dialogues Clin Neurosci 8:311–321.

Guedj F, Pereira PL, Najas S, Barallobre MJ, Chabert C, Souchet B, Sebrie C, Verney C, Herault Y, Arbones M, Delabar JM. 2012. DYRK1A: A master regulatory protein controlling brain growth. Neurobiol Dis 46:190–203.

Guedj F, Bianchi DW. 2013. Noninvasive prenatal testing creates an opportunity for antenatal treatment of Down syndrome. Prenat Diagn 33:614–618.

Guedj F, Bianchi DW, Delabar JM. 2014. Prenatal treatment of Down syndrome: A reality?. Curr Opin Obstet Gynecol 26:92–103.

Guedj F, Pennings JL, Wick HC, Bianchi DW. 2015. Analysis of adult cerebral cortex and hippocampus transcriptomes reveals unique molecular changes in the Ts1Cje mouse model of Down syndrome. Brain Pathol 25:11–23.

Guidi S, Ciani E, Bonasoni P, Santini D, Bartesaghi R. 2011. Widespread proliferation impairment and hypocellularity in the cerebellum of fetuses with Down syndrome. Brain Pathol 21:361–373.

Guidi S, Stagni F, Bianchi P, Ciani E, Ragazzi E, Trazzi S, Grossi G, Mangano C, Calza L, Bartesaghi R. 2013. Early pharmacotherapy with fluoxetine rescues dendritic pathology in the Ts65Dn mouse model of Down syndrome. Brain Pathol 23:129–143.

Guidi S, Stagni F, Bianchi P, Ciani E, Giacomini A, De Franceschi M, Moldrich R, Kurniawan N, Mardon K, Giuliani A, Calza L, Bartesaghi R. 2014. Prenatal pharmacotherapy rescues brain development in a Down's syndrome mouse model. Brain 137:380–401.

Guihard-Costa AM, Khung S, Delbecque K, Menez F, Delezoide AL. 2006. Biometry of face and brain in fetuses with trisomy 21. Pediatr Res 59: 33–38.

Hill JM, Lim MA, Stone MM. 2008. Developmental milestones in the newborn mouse. Neuromethods 39:131–149.

Holtzman DM, Santucci D, Kilbridge J, Chua-Couzens J, Fontana DJ, Daniels SE, Johnson RM, Chen K, Sun Y, Carlson E, Alleva E, Epstein CJ,

Mobley WC. 1996. Developmental abnormalities and age-related neurodegeneration in a mouse model of Down syndrome. Proc Natl Acad Sci USA 93:13333–13338.

Huang da W, Sherman BT, Lempicki RA. 2009. Systematic and integrative analysis of large gene lists using DAVID bioinformatics resources. Nat Protoc 4:44–57.

Huang H, Feng J, Famulski J, Rattner JB, Liu ST, Kao GD, Muschel R, Chan GK, Yen TJ. 2007. Tripin/hSgo2 recruits MCAK to the inner centromere to correct defective kinetochore attachments. J Cell Biol 177:413–424.

Ishihara K, Amano K, Takaki E, Shimohata A, Sago H, Epstein CJ, Yamakawa K. 2010. Enlarged brain ventricles and impaired neurogenesis in the Ts1Cje and Ts2Cje mouse models of Down syndrome. Cereb Cortex 20:1131–1143.

Johnson KL, Tao K, Stroh H, Kallenbach L, Peter I, Richey L, Rust D, Bianchi DW. 2010. Increased fetal cell trafficking in murine lung following complete pregnancy loss from exposure to lipopolysaccharide. Fertil Steril 93:1718–1721. e2.

Jursky F, Nelson N. 1996. Developmental expression of the glycine transporters GLYT1 and GLYT2 in mouse brain. J Neurochem 67:336–344.

Kahlem P, Sultan M, Herwig R, Steinfath M, Balzereit D, Eppens B, Saran NG, Pletcher MT, South ST, Stetten G, Lehrach H, Reeves RH, Yaspo ML. 2004. Transcript level alterations reflect gene dosage effects across multiple tissues in a mouse model of Down syndrome. Genome Res 14:1258–1267.

Laffaire J, Rivals I, Dauphinot L, Pasteau F, Wehrle R, Larrat B, Vitalis T, Moldrich RX, Rossier J, Sinkus R, Herault Y, Dusart I, Potier MC. 2009. Gene expression signature of cerebellar hypoplasia in a mouse model of Down syndrome during postnatal development. BMC Genomics 10:138–2164-10-138.

Ling KH, Hewitt CA, Tan KL, Cheah PS, Vidyadaran S, Lai MI, Lee HC, Simpson K, Hyde L, Pritchard MA, Smyth GK, Thomas T, Scott HS. 2014. Functional transcriptome analysis of the postnatal brain of the Ts1Cje mouse model for Down syndrome reveals global disruption of interferon-related molecular networks. BMC Genomics 15:624–2164-15-624.

Lockstone HE, Harris LW, Swatton JE, Wayland MT, Holland AJ, Bahn S. 2007. Gene expression profiling in the adult Down syndrome brain. Genomics 90:647–660.

Mao R, Wang X, Spitznagel EL Jr, Frelin LP, Ting JC, Ding H, Kim JW, Ruczinski I, Downey TJ, Pevsner J. 2005. Primary and secondary transcriptional effects in the developing human Down syndrome brain and heart. Genome Biol 6:R107.1–R107.20.

Mao R, Zielke CL, Zielke HR, Pevsner J. 2003. Global up-regulation of chromosome 21 gene expression in the developing Down syndrome brain. Genomics 81:457–467.

Marchal JA, Ghani M, Schindler D, Gavvovidis I, Winkler T, Esquitino V, Sternberg N, Busche A, Krawitz P, Hecht J, Robinson P, Mundlos S, Graul-Neumann L, Sperling K, Trimborn M, Neitzel H. 2011. Misregulation of mitotic chromosome segregation in a new type of autosomal recessive primary microcephaly. Cell Cycle 10:2967–2977.

Mohler H, Boison D, Singer P, Feldon J, Pauly-Evers M, Yee BK. 2011. Glycine transporter 1 as a potential therapeutic target for schizophrenia-related symptoms: Evidence from genetically modified mouse models and pharmacological inhibition. Biochem Pharmacol 81:1065–1077.

Moldrich RX, Dauphinot L, Laffaire J, Vitalis T, Herault Y, Beart PM, Rossier J, Vivien D, Gehrig C, Antonarakis SE, Lyle R, Potier MC. 2009. Proliferation deficits and gene expression dysregulation in Down's syndrome (Ts1Cje) neural progenitor cells cultured from neurospheres. J Neurosci Res 87:3143–3152.

Nie J, Wang H, He F, Huang H. 2010. Nusap1 is essential for neural crest cell migration in zebrafish. Protein Cell 1:259–266.

Olson LE, Roper RJ, Baxter LL, Carlson EJ, Epstein CJ, Reeves RH. 2004. Down syndrome mouse models Ts65Dn, Ts1Cje, and Ms1Cje/Ts65Dn exhibit variable severity of cerebellar phenotypes. Dev Dyn 230:581–589.

Potier MC, Rivals I, Mercier G, Ettwiller L, Moldrich RX, Laffaire J, Personnaz L, Rossier J, Dauphinot L. 2006. Transcriptional disruptions in Down syndrome: A case study in the Ts1Cje mouse cerebellum during post-natal development. J Neurochem 97:104–109.

Purdy IB, Singh N, Brown WL, Vangala S, Devaskar UP. 2014. Revisiting early hypothyroidism screening in infants with Down syndrome. J Perinatol 34:936–940.

Rask-Andersen M, Masuram S, Fredriksson R, Schioth HB. 2013. Solute carriers as drug targets: Current use, clinical trials and prospective. Mol Aspects Med 34:702–710.

Rieder CL, Salmon ED. 1998. The vertebrate cell kinetochore and its role during mitosis. Trends Cell Biol 8:310–318.

Santamaria D, Ortega S. 2006. Cyclins and CDKS in development and cancer: Lessons from genetically modified mice. Front Biosci 11: 1164–1188.

Santucci D, Calamandrei G, Alleva E. 1993. Neonatal exposure to bFGF exerts NGF-like effects on mouse behavioral development. Neurotoxicol Teratol 15:131–137.

Saran NG, Pletcher MT, Natale JE, Cheng Y, Reeves RH. 2003. Global disruption of the cerebellar transcriptome in a Down syndrome mouse model. Hum Mol Genet 12:2013–2019.

Satoh J, Kawana N, Yamamoto Y. 2013. Pathway analysis of ChIP-seq-based NRF1 target genes suggests a logical hypothesis of their involvement in the pathogenesis of neurodegenerative diseases. Gene Regul Syst Bio 7:139–152.

Schick V, Majores M, Fassunke J, Engels G, Simon M, Elger CE, Becker AJ. 2007. Mutational and expression analysis of CDK1, cyclinA2 and cyclinB1 in epilepsy-associated glioneuronal lesions. Neuropathol Appl Neurobiol 33:152–162.

Schmidt-Sidor B, Wisniewski KE, Shepard TH, Sersen EA. 1990. Brain growth in Down syndrome subjects 15 to 22 weeks of gestational age and birth to 60 months. Clin Neuropathol 9:181–190.

Sczaniecka MM, Hardwick KG. 2008. The spindle checkpoint: How do cells delay anaphase onset?. SEB Exp Biol Ser 59:243–256.

Singer P, Feldon J, Yee BK. 2009. The glycine transporter 1 inhibitor SSR504734 enhances working memory performance in a continuous delayed alternation task in C57BL/6 mice. Psychopharmacology (Berl) 202:371–384.

Slonim DK, Koide K, Johnson KL, Tantravahi U, Cowan JM, Jarrah Z, Bianchi DW. 2009. Functional genomic analysis of amniotic fluid cell-free mRNA suggests that oxidative stress is significant in Down syndrome fetuses. Proc Natl Acad Sci USA 106:9425–9429.

Stewart ZA, Westfall MD, Pietenpol JA. 2003. Cell-cycle dysregulation and anticancer therapy. Trends Pharmacol Sci 24:139–145.

Subramanian A, Tamayo P, Mootha VK, Mukherjee S, Ebert BL, Gillette MA, Paulovich A, Pomeroy SL, Golub TR, Lander ES, Mesirov JP. 2005. Gene set enrichment analysis: A knowledge-based approach for interpreting genome-wide expression profiles. Proc Natl Acad Sci USA 102:15545–15550.

Takahashi A, Yap JJ, Bohager DZ, Faccidomo S, Clayton T, Cook JM, Miczek KA. 2009. Glutamatergic and GABAergic modulations of ultrasonic vocalizations during maternal separation distress in mouse pups. Psychopharmacology (Berl) 204:61–71.

Van Trotsenburg AS, Vulsma T, van Santen HM, Cheung W, de Vijlder JJ. 2003. Lower neonatal screening thyroxine concentrations in Down syndrome newborns. J Clin Endocrinol Metab 88:1512–1515.

Weick JP, Held DL, Bonadurer GF, Doers 3rd, Liu ME, Maguire Y, Clark C, Knackert A, Molinarolo JA, Musser K, Yao M, Yin L, Lu Y, Zhang J, Zhang X, Bhattacharyya SC, . 2013. Deficits in human trisomy 21 iPSCs and neurons. Proc Natl Acad Sci USA 110:9962–9967.

Winter TC, Ostrovsky AA, Komarniski CA, Uhrich SB. 2000. Cerebellar and frontal lobe hypoplasia in fetuses with trisomy 21: Usefulness as combined US markers. Radiology 214:533–538.

Wohr M, Scattoni ML. 2013. Behavioural methods used in rodent models of autism spectrum disorders: Current standards and new developments. Behav Brain Res 251:5–17.

Yang YT, Wang CL, Van Aelst L. 2012. DOCK7 interacts with TACC3 to regulate interkinetic nuclear migration and cortical neurogenesis. Nat Neurosci 15:1201–1210.

Yee BK, Balic E, Singer P, Schwerdel C, Grampp T, Gabernet L, Knuesel I, Benke D, Feldon J, Mohler H, Boison D. 2006. Disruption of glycine transporter 1 restricted to forebrain neurons is associated with a pro-cognitive and antipsychotic phenotypic profile. J Neurosci 26: 3169–3181.

SUPPORTING INFORMATION

Additional supporting information may be found in the online version of this article at the publisher's web-site.